Positive shift of Na$_v$1.8 current inactivation curve in injured neurons causes neuropathic pain following chronic constriction injury

GUIXIA LI, XIFANG LIU, JINGNAN DU, JIANZHAO CHEN, FENGLIN SHE, CHUNFU WU and CHUNLI LI

Department of Pharmacology, Shenyang Pharmaceutical University, Shenyang, Liaoning 110016, P.R. China

Abstract. Neuropathic pain is a global medical concern, characterized by spontaneous pain, heat hyperalgesia and mechanical allodynia. The condition has been associated with alterations in the voltage-gated sodium channels, Na$_v$1.8 and Na$_v$1.9, in nociceptive neurons termed nociceptors. However, an explanation for the contribution of these channels to the phenotype observed in neuropathic pain remains to be elucidated. The changes induced by chronic constriction injury (CCI) to Na$_v$1.8 and Na$_v$1.9 mRNA and protein levels, as well as electrical currents in injured and contralateral non-injured dorsal root ganglion (DRG) neurons are described in the present study. A marked downregulation was observed for each Na$_v$ isoform transcript and protein expressed in injured neurons with the exception of the Na$_v$1.9 protein, which exhibited no change, while in contralateral non-injured neurons, the levels of protein and mRNA remained unchanged. Na$_v$ isoform functional analysis was then performed in L$_{4-6}$ DRG neurons 14 days after CCI. The Na$_v$1.8 current density was markedly decreased in injured DRG neurons following CCI. The voltage-dependent activation of the Na$_v$1.8 channel in these neurons was shifted to depolarized potentials by 5.3 mV, while it was shifted to hyperpolarized potentials by 10 mV for inactivation. The electrophysiological function of Na$_v$1.9 was not affected by CCI. The present study demonstrated that ectopic discharge following CCI, which was likely induced by a positive shift in the Na$_v$1.8 current inactivation curve in injured neurons, enhanced the excitability of the neurons by facilitating tetrodotoxin-resistant sodium channels into the fast inactivation state and did not occur as a result of a compensatory redistribution in the contralateral uninjured neurons.

Correspondence to: Dr Chunli Li or Dr Chunfu Wu, Department of Pharmacology, Shenyang Pharmaceutical University, 103 Wenhua Road, Shenyang, Liaoning 110016, P.R. China
E-mail: lichunli_2014@126.com
E-mail: wucf@syphu.edu.cn

Introduction

Neuropathic pain is an unmet medical concern, affecting individuals globally. The condition has been causally correlated with functional alterations in the sodium channels of nociceptors (1). Sodium channels are integral membrane glycoproteins, which are responsible for the generation and conduction of action potentials in excitable cells (2). Previous studies have revealed that sodium channel blockers, including local anesthetics, tricyclics and certain anti-convulsants, are able to attenuate pain in patients with neural injury (3,4). The voltage-gated sodium channel isoforms, Na$_v$1.8 and Na$_v$1.9, encoding for slowly-gating tetrodotoxin-resistant (TTX-R) sodium currents, are particularly notable with respect to sensory nerve pathophysiology. They are sensory neuron-specific with Na$_v$1.8 expressed in thinly unmyelinated (C-fibers) and 10% myelinated (A-fibers) axons. By contrast, the expression of Na$_v$1.9 is restricted to small C-fiber dorsal root ganglion (DRG) cells (5). Differential expression of these sodium channels is coupled with isoform-specific contributions in neuronal excitability and the transmission of sensory information (6). Na$_v$1.8 produces the majority of the depolarizing inward current during an action potential (7), while Na$_v$1.9 has been proposed to contribute to maintaining the resting potential (8). The absence of these channels in the central nervous system implicates them as a suitable target for therapeutic intervention in pain management with few side effects (2).

Peripheral nerve injury, for example axotomy or nerve transection, causes a downregulation of Na$_v$1.8 expression and a decrease in the electrical current attributed to this channel in injured neurons (3,9,10). Additionally, specific knockdown of Na$_v$1.8 with antisense oligodeoxynucleotides may effectively reverse neuropathic pain (11). However, it is not intuitively clear how this contributes to the neuropathic pain phenotype associated with these models. Previous studies have observed that upregulation of the expression of Na$_v$1.8 in spared neurons following nerve injury, with the exception of chronic constriction injury (CCI) or spared nerve injury models, may provide a reasonable explanation for the contribution of this channel to the pain phenotype (10,12-14). In addition, there are specific discrepancies in the evidence among studies with regards to the involvement of Na$_v$1.9 in certain neuropathic pain conditions (2,15-17). The expression of Na$_v$1.9 is downregulated

in injured DRG neurons (15) and is upregulated in uninjured neurons following peripheral nerve injury (16), while abnormal behavior in the Na$_v$1.9 knockout mouse remains unchanged in neuropathic pain models (2). To resolve this limitation, a CCI model was established in the present study to evaluate whether Na$_v$1.8 sodium channels mediate neuropathic pain through a compensatory redistribution to contralateral uninjured DRG neurons and to elucidate the exact role of Na$_v$1.9 in neuropathic pain.

Materials and methods

Experimental animals. A total of 72 adult male Sprague-Dawley rats weighing 150-180 g and aged 6-8 weeks, purchased from the Experimental Animal Centre of Shenyang Pharmaceutical University (Shenyang, China), were used in all experiments. Rats were maintained under controlled environmental conditions at 23±2°C with a 12-h light/dark cycle and *ad libitum* access to food and water. All procedures were performed in accordance with the guidelines of the International Association for the Study of Pain (18). The study was approved by the ethics committee of Shenyang Pharmaceutical University.

CCI model. The CCI model was induced as previously described (19,20). Briefly, under anesthesia with 3.5% chloral hydrate (10 ml/kg; Hebei Gaobeidian Chunguang Chemical Reagent Company, Gaobeidian, China) administered intraperitoneally (i.p.), the right sciatic nerve was exposed and loosely ligated with 4-0 chromic catgut (Shanghai Pudong Medical Supplies Co., Ltd., Shanghai, China) in four regions separated by ~1 mm, then the incision was closed with sutures. For the sham group, the right sciatic nerve was exposed without ligation. Pain-associated behavioral assessments were performed at the time-points of: -1 (prior to CCI surgery), 1, 3, 5, 7, 10, 14 and 21 days after CCI surgery.

Behavioral assessment. The abnormal posture of each animal was evaluated using a subjective pain-associated behavioral grade as described previously (21) by an investigator who was blinded to the experimental conditions. Briefly, grades were determined as: 0, normal; 1, coiling of the toes; 2, valgus deformity of the paw; 3, partially weight bearing; 4, non-weight bearing and 5, avoidance of any contact with the hind paw.

Paw withdrawal response to thermal stimuli. The paw withdrawal response was measured using the Plantar Test meter (IITC Life Science Inc., Woodland Hills, CA, USA). Rats were placed individually in a clear, transparent box (17x11.5x14 cm) and allowed to acclimate for 15 min prior to the assessment. An infrared beam of a radiant heat source was applied to irradiate the plantar surface of the hind paw through the glass plate until the rat withdrew or contracted its paw. The withdrawal thresholds were measured in each hind paw and the ipsilateral hind paw was assessed at 15 min intervals, while the contralateral hind paw was assessed at 5 min intervals. A 20 sec limit was imposed to prevent tissue damage. Each rat was assessed five times and the mean value was expressed as the thermal withdrawal latency (22).

The paw withdrawal response to mechanical stimuli was measured using the Electronic von Frey Anesthesiometer

(IITC Life Science Inc.). Rats were placed individually into wire mesh-bottom boxes (20x14x16 cm) and allowed to acclimate for 30 min prior to assessment. The probe was placed beneath the plantar surface of the hind paw and the force was increased until the rat was observed to vellicate its paw. The maximum force was recorded at the time of paw withdrawal. Withdrawal thresholds were measured in each hind paw and the ipsilateral hind paw was assessed at 30 sec intervals, while the contralateral hind paw was assessed at 15 sec intervals. Each rat was assessed five times and the average value was expressed as the mechanical withdrawal threshold (23).

Immunofluorescence and hematoxylin and eosin (H&E) staining. L$_{4-6}$ DRGs, quickly dissected from recently sacrificed animals, were fixed with 10% formalin overnight at 4°C. Following embedding the tissue in paraffin, a series of 5-μm sections were cut for immunofluorescence and H&E staining. Paraffin sections were treated with dimethylbenzene solution I for 15 min, dimethylbenzene solution II for 15 min, dimethylbenzene:pure ethanol (1:1) solution for 2 min, 100% ethanol I for 5 min, 100% ethanol II for 5 min, 95% ethanol solution for 3 min, 90% ethanol solution for 1 min, 85% ethanol solution for 1 min, 75% ethanol solution for 1 min, 50% ethanol solution for 1 min, running water for 2 min, haematoxylin solution for 2 min, running water for 1 min, 1% hydrochloric acid ethanol solution for 20 sec, running water for 5 min, Eosin solution for 30 sec, running water for 30 sec, 75% ethanol solution for 30 sec, 85% ethanol solution for 20 sec, 95% ethanol solution I for 1 min, 95% ethanol solution II for 1 min, 100% ethanol for 2 min, 100% ethanol II for 2 min, dimethylbenzene solution I for 2 min, dimethylbenzene solution II for 2 min then dimethylbenzene solution III for 2 min. The primary antibodies polyclonal rabbit Na$_v$1.8 (ASC-016; 1:200; Alomone Laboratories Ltd., Jerusalem, Israel), monoclonal mouse neurofilament (NF)200 (N0142; 1:200; Sigma-Aldrich, St. Louis, MO, USA) and polyclonal rabbit Na$_v$1.9 (ASC-017; 1:200; Alomone Laboratories Ltd.) were administered for immunofluorescence staining and used to incubate the sections overnight at 4°C. Following three washes with phosphate-buffered saline containing Tween-20, the sections were incubated with anti-mouse IgG fluorescein isothiocyanate-conjugated antibody produced in goat (F0257) and anti-rabbit IgG (whole molecule)-Cy3 antibody produced in sheep (C2306) (1:100; Sigma-Aldrich) for 1 h at 37°C. Images were captured under an inverted fluorescence microscope (Olympus BX40; Olympus, Tokyo, Japan) and imported into Image pro plus 6.0 software (Media Cybernetics, Silver Spring, MD, USA) for further analysis. H&E staining was performed according to the manufacturer's instructions (Sigma-Aldrich). Nuclear material within the nucleus was stained a deep purple/blue, while the cytoplasmic material, including connective tissue and collagen appeared orange/pink.

Reverse transcription-quantitative polymerase chain reaction (RT-qPCR). At 3, 7, 14 and 21 days after CCI, rats were sacrificed via anesthesia with 3.5% chloral hydrate (10 ml/kg, i.p.). The ipsilateral and contralateral L$_{4-6}$ DRGs were rapidly removed and placed into Eppendorf tubes. Total RNA was extracted using TRIzol reagent (Invitrogen Life Technologies,

Carlsbad, CA, USA) and the cDNA was reverse transcribed using the PrimeScript® RT reagent kit (Takara Bio Inc., Otsu, Japan) according to the manufacturer's instructions. PCR was performed in a 25-μl reaction mixture containing 2 μl templates, 12.5 μl SYBR® Premix Ex Taq™ (2X), 0.5 μl ROX reference dye II (50X) and 0.4 μM primer for each gene. The thermal cycling conditions comprised 30 sec polymerase activation at 95°C, 40 cycles of 15 sec denaturation at 95°C and 1 min at 60°C for annealing and extension. A dissociation curve was used to determine the amplification specificity. The primer sequences (24) were as follows: $Na_v1.8$ (GenBank accession number, U53833) forward, 5'-GACTCCCGGACAAATCAGAA-3' and reverse, 5'-AGCAGCGACCTCATCTTCAT-3'; $Na_v1.9$ (GenBank accession number, AF059030) forward, 5'-TCTCCACCCCTACCTCACTG-3' and reverse, 5'-CGTTCAGCCAAAAACACAGA-3'; and GAPDH forward, 5'-TGCCAAGTATGATGACATCAAGAAG-3' and reverse, 5'-AGCCCAGGATGCCCTTTAGT-3'. The threshold cycle values of $Na_v1.8$ and $Na_v1.9$ mRNA were measured and normalized to GAPDH, and then expressed as a relative ratio. The Mx3000P qPCR system was used (Agilent Technologies, Inc., Santa Clara, CA, USA).

Western blot analysis. Bilateral L_{4-6} DRGs were dissected and total proteins were extracted via homogenization in ice-cold lysate buffer (Thermo Fisher Scientific, Waltham, MA, USA). Samples (30-50 μg) were separated on 8% SDS-PAGE separation gels (Amresco, Boise ID, USA) and subsequently transferred onto polyvinylidene difluoride membranes (Merck Millipore, Boston, MA, USA). The membranes were blocked in 5% skimmed milk solution at room temperature for 2 h and then rabbit polyclonal $Na_v1.8$ (1:500; Alomone Laboratories Ltd.), $Na_v1.9$ (1:500; Alomone Laboratories Ltd.) and mouse monoclonal β-actin (1:500; Santa Cruz Biotechnology, Inc., Dallas, TX, USA) primary antibodies were used to incubate the samples overnight at 4°C. The target bands were detected with secondary horseradish peroxidase (HRP)-labeled goat anti-rabbit (1:10,000; ZB-2301) or HRP-labeled goat anti-mouse IgG (1:5,000; ZB2305) (Zhongshan Golden Bridge Biotechnology Co., Ltd., Beijing, China) antibodies for 1 h at room temperature. The band intensity of $Na_v1.8$ and $Na_v1.9$ was normalized to that of β-actin and expressed as a relative ratio.

Patch clamp recording. Rat DRG neurons were acutely dissociated as previously described (25). The samples were superfused at a rate of 3 ml/min and all patch clamp recordings were performed using an Axopatch 200B amplifier (Molecular Devices, Sunnyvale, CA, USA), filtered at 1 kHz and digitally sampled at 10 kHz at room temperature (23±2°C). Clampfit 10.0 software (Molecular Devices) was used for data acquisition and analysis.

The bath solution for the $Na_v1.8$ currents contained (in mM): 140 NaCl, 1 $MgCl_2$, 3 $CaCl_2$, 5 KCl (Tianjin Bodi Chemical Co. Ltd., Tianjin, China), 10 tetraethylammonium (TEA)-Cl, 1 4-aminopyridine, 0.2 $CdCl_2$, 10 4-(2-hydroxyethyl)-1-piperazineethanesulfonic acid (HEPES), 10 glucose (Tianjin Bodi Chemical Co. Ltd.), 0.001 TTX (Hebei Fisheries Research Institute, Qinhuangdao, China), pH 7.3 with NaOH (Tianjin Bodi Chemical Co. Ltd.). The bath solution for the $Na_v1.9$
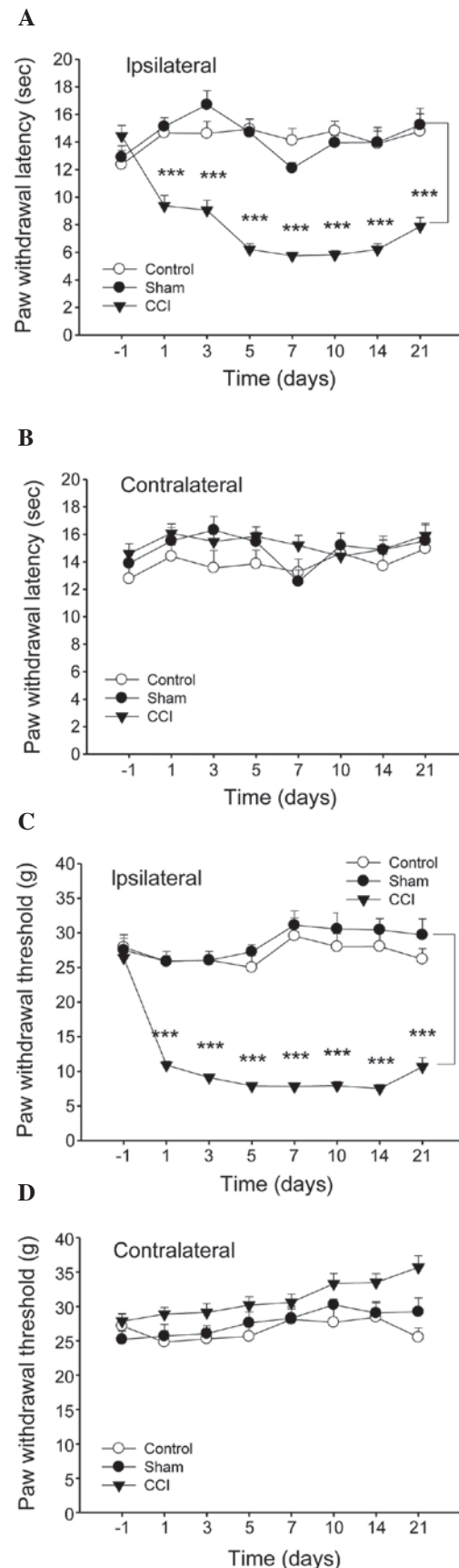

Figure 1. CCI-induced neuropathic pain evokes heat hyperalgesia and mechanical allodynia. (A and C) Significant decreases in the ipsilateral mean paw withdrawal latency and mean paw withdrawal threshold were observed from day 1 and persisted for 21 days. (B and D) Contralateral paw withdrawal. Values are expressed as the mean ± standard error of the mean. *P<0.05; ***P<0.001 vs. sham group. CCI, chronic constriction injury.
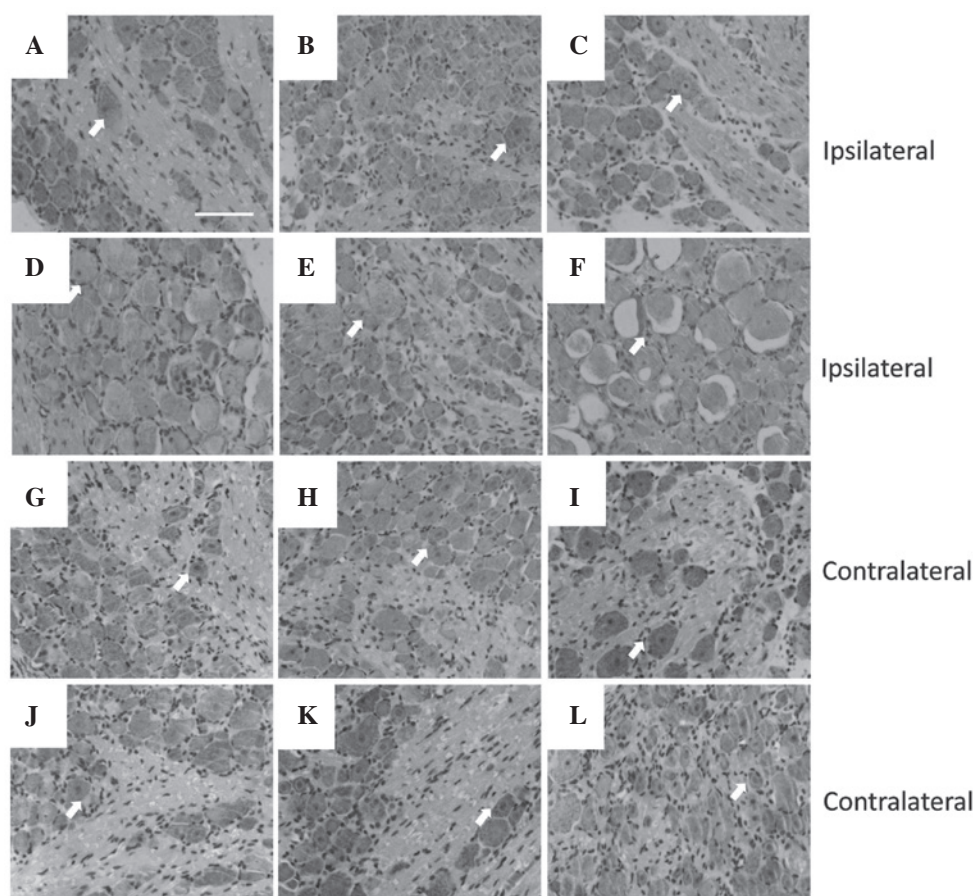
Figure 2. Micrographs of H&E staining in representative L$_{4-6}$ DRG slices. Representative sections stained with H&E revealed a gradual injury (arrow) in ipsilateral DRG cells at the point of (C) 3, (D) 7, (E) 14 and (F) 21 days after CCI compared with the sham group (B). Normal cellular morphology is shown in (A) the control and (B) the sham group ipsilateral and (G-L) in the other groups' contralateral L$_{4-6}$ DRG of rats. Scale bar, 50 μm. H&E, hematoxylin and eosin; DRG, dorsal root ganglion; CCI, chronic constriction injury.

currents contained 30 NaCl, 20 TEA-Cl, 90 choline chloride, 3 KCl, 1 CaCl$_2$, 1 MgCl$_2$, 10 HEPES, 10 glucose, 0.1 CdCl$_2$, 0.001 TTX, pH 7.3 with Tris base (all purchased from Sigma-Aldrich unless specified). The pipette solution used for recording the DRG neuron Na$_v$1.8 and Na$_v$1.9 currents contained (in mM): 140 CsCl, 10 TEA-Cl, 10 ethylene glycol tetraacetic acid (EGTA; Amresco), 10 HEPES, pH 7.2 with CsOH and 135 CsF, 10 NaCl, 10 HEPES, 5 EGTA, 2 adenosinetriphosphate bisodium, pH 7.2 with CsOH, respectively. The pipettes, fabricated with a P-97 puller (Sutter Instruments, Novato, CA, USA), had resistances of 3-5 MΩ when filled with pipette solution.

Statistical analysis. Data were analysed using SPSS 16.0 (SPSS, Inc., Chicago, IL, USA) with a one-way analysis of variance. All measurements are expressed as the mean ± standard error. P<0.05 was considered to indicate a statistically significant difference.

Results

CCI-induced neuropathic pain evokes spontaneous pain, mechanical allodynia and heat hyperalgesia. The CCI model induced the typical features of neuropathic pain, which were assessed via behavioral grade, the Plantar Test meter and the Electronic von Frey Anesthesiometer. Rats with nerve injury

(CCI) exhibited curling, eversion, partial weight bearing or non-weight bearing on the right injured side, while they exhibited normal behavior on the left uninjured paw. The score for the right paw increased significantly from the first day after surgery (data not shown).

The sensitivity to heat and mechanical stimulus revealed certain discrepancies among the experimental groups. In the CCI model group, the thermal withdrawal latency and mechanical withdrawal threshold of the right injured paw decreased markedly from day 1 after injury, with the maximal level of hypersensitivity at 7 days after surgery, while observable changes were not observed in the sham surgery group (Fig. 1A and C). By contrast, no differences were observed in the contralateral paw withdrawal in all groups (Fig. 1B and D).

CCI-induced neuropathic pain impairs DRG histological morphology. In peripheral nerve injury, the majority of neuronal cell death is observed in peripheral nerve lesions, which are considered to be a major factor in the poor clinical outcome following the injury (26). With H&E staining, ipsilateral and contralateral DRGs to the injury (Fig. 2) were analyzed histologically. In each contralateral DRG group (Fig. 2G-L), the neurons exhibited a normal cellular appearance, including a large, round nucleus, clear cell boundaries and even chromatin distribution. However, neurons on the ipsi-
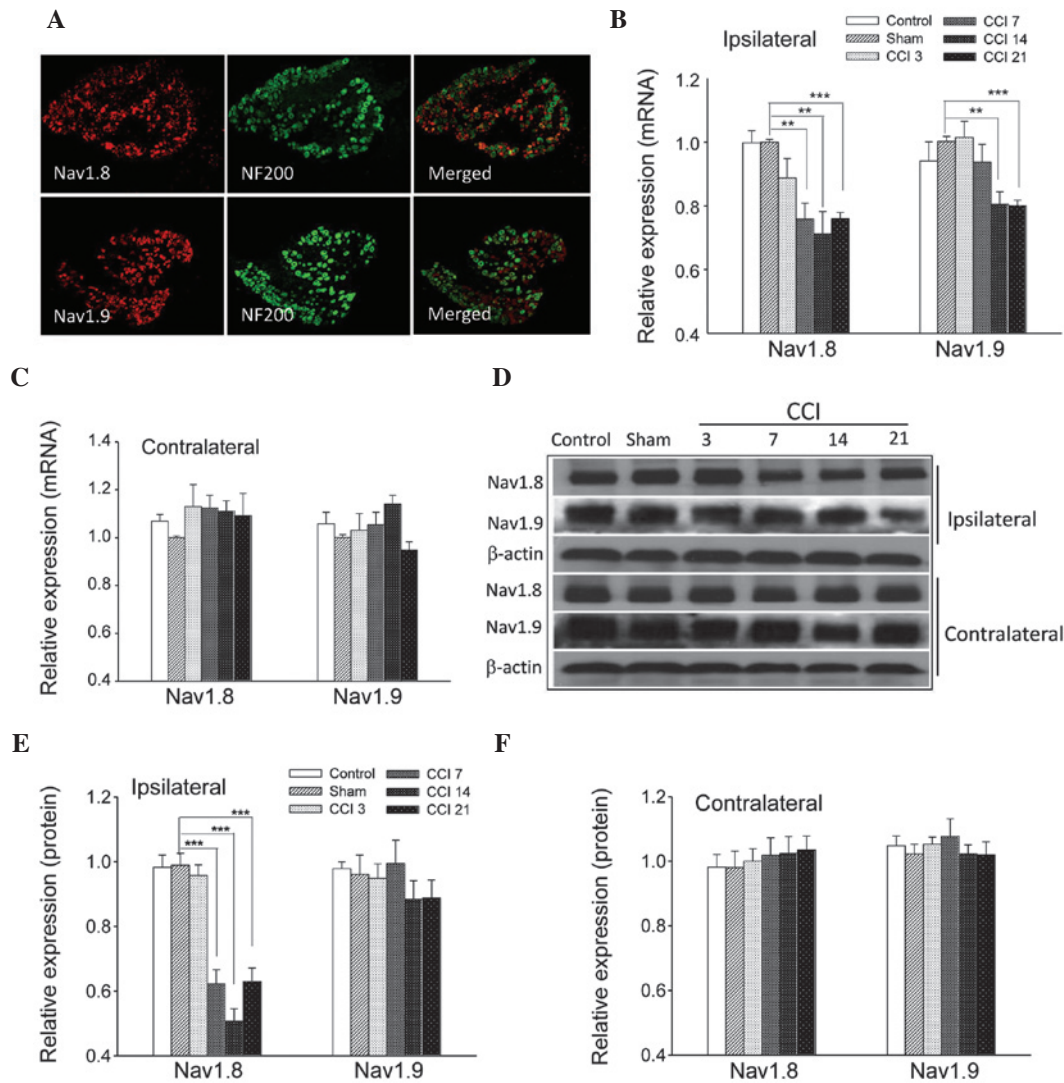
Figure 3. Changes in the expression and distribution of $Na_v1.8$ and $Na_v1.9$ following CCI. (A) DRG sections were labeled with anti-NF200, anti-$Na_v1.8$ and anti-$Na_v1.9$ antibodies. (B) $Na_v1.8$ mRNA levels were significantly decreased in ipsilateral DRGs at 7, 14 and 21 days, while $Na_v1.9$ expression was markedly lower at 14 and 21 days after CCI. (C) Relative expression of $Na_v1.8$ and $Na_v1.9$ mRNA in contralateral DRGs. (D) Representative images of $Na_v1.8$ and $Na_v1.9$ protein and (E and F) relative ratio of $Na_v1.8$ protein exhibited a significant decrease at 7-21 days after CCI in ipsilateral DRGs. Values are expressed as the mean ± standard error of the mean. **P<0.01; ***P<0.001, vs. sham group. DRG, dorsal root ganglion; CCI, chronic constriction injury; NF200, neurofilament 200.

lateral side to the injury exhibited a range of morphologies at different time-points (Fig. 2C-F), although all observed cells had abnormal nuclei exhibiting pyknosis, membrane irregularities or even vacuolation, with the maximal magnitude of neuronal death at 21 days after surgery.

Expression profiles of $Na_v1.8$ and $Na_v1.9$ in DRG neurons under CCI-induced neuropathic pain. The neurofilament NF200 is preferentially expressed in large DRG neurons and is a useful marker for this population (7). When co-incubated with antibodies against $Na_v1.8$ and $Na_v1.9$ in an immunofluorescence assay, it was observed that $Na_v1.8$ and $Na_v1.9$ subunits were primarily located in the small and medium diameter DRG neurons (Fig. 3A).

RT-qPCR and western blot analyses were performed at 3, 7, 14 and 21 days after the CCI surgery instead of at an earlier point, in order to avoid potential error due to the effects of post-surgical pain. CCI induced a marked downregulation of the $Na_v1.8$ transcript at 7 days (0.76±0.05; P<0.01), 14 days

(0.71±0.07; P<0.01) and 21 days (0.76±0.02; P<0.001) and a substantial downregulation of $Na_v1.9$ transcript at 14 days (0.81±0.04; P<0.01) and 21 days (0.806±0.02; P<0.001) in L_{4-6} ipsilateral DRGs (Fig. 3B); however, no significant differences were observed among groups in the contralateral DRGs (Fig. 3C; P>0.05). Representative images of $Na_v1.8$ and $Na_v1.9$ protein expression within the ipsilateral and contralateral DRGs are shown in Fig. 3D. Consistent with these findings, RT-qPCR analysis revealed that the relative ratio of band intensity of $Na_v1.8$ protein in ipsilateral DRGs was significantly reduced at 7 days (0.62±0.04; P<0.001), 14 days (0.51±0.04; P<0.001) and 21 days (0.63±0.04; P<0.001) after CCI treatment, while $Na_v1.9$ protein expression following CCI exhibited a decrease at 14 days (0.88±0.06; P>0.05) and 21 days (0.89±0.06, P>0.05; Fig. 3E). However, the differences were not statistically significant when compared with the sham group. In addition, there were no detectable differences among contralateral DRG neurons from the rats subjected to CCI (Fig. 3F). These results markedly suggested that $Na_v1.8$

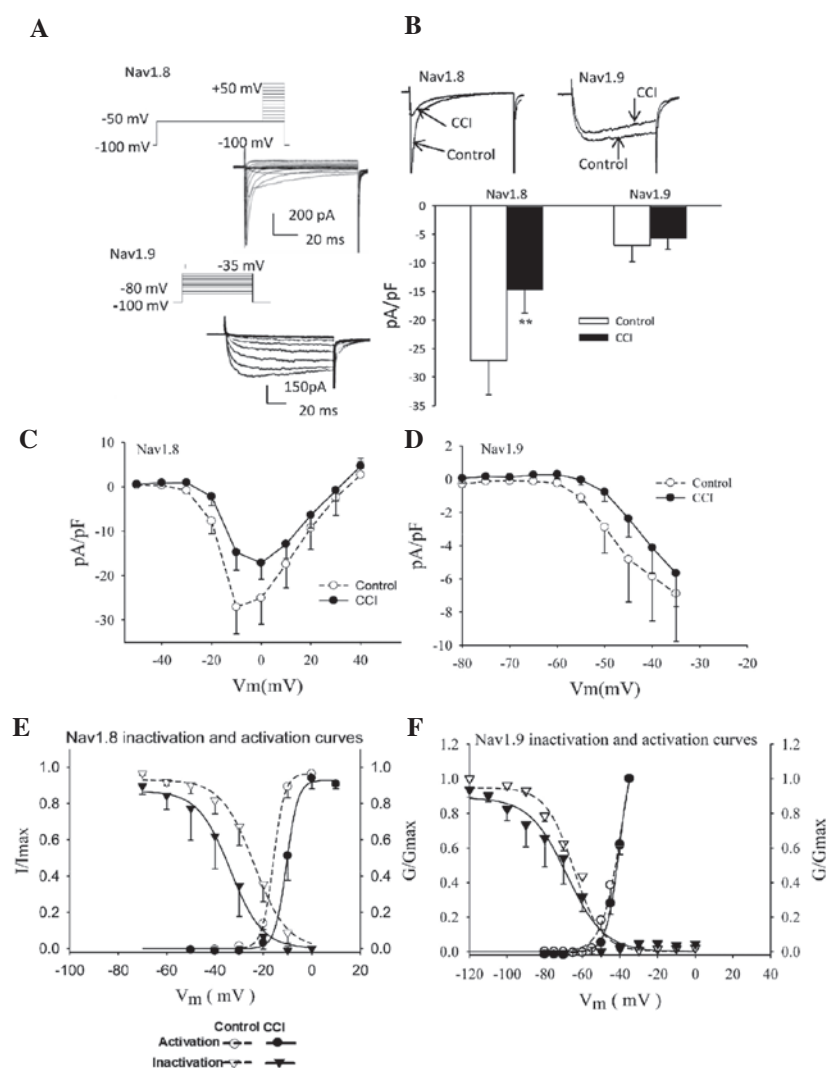Figure 4. Changes in Na$_v$1.8 and Na$_v$1.9 electrophysiological functions following CCI treatment. (A) Na$_v$1.8 current was evoked by depolarizing voltage steps between -50 and +50 mV in 10-mV increments from a holding potential of -100 mV. The current of Na$_v$1.9 was generated by 5-mV progressive steps between -80 and -35 mV from a holding potential of -100 mV. (B) Following CCI surgery, the peak sodium current density mediated by Na$_v$1.8 was significantly decreased by ~50% (P<0.01). (C and D) The average amplitude of the Na$_v$1.8 and Na$_v$1.9 sodium currents as a function of test pulse voltage in DRG neurons exhibited no change. (E) Dynamics investigations revealed that CCI treatment caused a depolarizing shift of 5.3 mV in the activation curve and ~10 mV positive shift of the inactivation curve of Na$_v$1.8. (F) However, no significant difference was identified between injured and control DRG neurons with regard to the biophysical properties of Na$_v$1.9. DRG, dorsal root ganglion; CCI, chronic constriction injury.

and Na$_v$1.9 sodium channels have distinct roles following CCI treatment.

Effect of CCI on TTX-R sodium channels in rat DRG neurons. The small- and medium-diameter DRG neurons (12-25 μm) were selected as the main focus of the present study. Differences in the voltage protocols and pharmacological inhibition by TTX were used to evoke Na$_v$1.8 and Na$_v$1.9 inward currents (Fig. 4A). Following CCI surgery, the sodium current densities mediated by Na$_v$1.8 and Na$_v$1.9 decreased ~50% (Fig. 4B; between -27.10±6.03 and -14.75±4.01 pA/pF; P<0.01) and 18% (Fig. 4B; between -6.90±2.89 and -5.67±2.00 pA/pF; P>0.05), respectively.

Steady-state activation curves were constructed as described from current-voltage curve experiments. The normalized activation curves of Na$_v$1.8 and Na$_v$1.9 were fitted with the Boltzmann function expressed as: $G/G_{max} = 1/\{1+exp[(V-V_{1/2})/K]\}$, where $V_{1/2}$ is the membrane

potential at half-activation and K represents the slope factor. Characterization of activation curves revealed that CCI treatment caused a depolarizing shift of 5.3 mV and 1.44 mV in Na$_v$1.8 (Fig. 4E; $V_{1/2}$ between -15.84±0.21 and -10.51±0.24 mV) and Na$_v$1.9 (Fig. 4F; between -40.28±1.02 mV and -38.84±2.07 mV) steady-state activation curves, respectively.

The voltage-dependent inactivation of the Na$_v$1.8 current is shown in Fig. 4E. The solid lines were fitted with the Boltzmann equation, $I/I_{max} = 1/\{1+exp[(V-V_{1/2})/K]\}$, where $V_{1/2}$ is the membrane potential when $I/I_{max} = 0.5$ and K represents the slope factor. There was a 10-mV depolarizing shift in the midpoint of inactivation (Fig. 4E; between -23.85±0.74 and -33.73±0.91 mV). This change reflected a parallel shift in the availability curve of the current as no change was observed in the slope factor (between -6.82±0.63 mV and -6.64±0.76 mV). However, no significant differences were identified between injured and control DRG neurons with respect to the biophysical properties of Na$_v$1.9 (Fig. 4F).

Discussion

Neuropathic pain originating from pathology within the nervous system is a serious unmet medical concern. Animal models of neuropathic pain, although often unrepresentative, provide important information for understanding the underlying mechanism of neuropathic pain in humans (27). Peripheral nerve injury may result in pain-associated behavior characterized by spontaneous pain, hyperalgesia and allodynia (28). CCI, as a classical neuropathic pain model, is able to induce spontaneous pain and hyperalgesia through noxious thermal and mechanical stimuli (29). In the present study, it has been demonstrated that CCI is able to stably induce the typical features of neuropathic pain. This method exhibited multiple advantages, including a simple surgical procedure with little tissue damage and a high success rate, with evident and stable spontaneous pain following surgery.

The present findings confirmed the results of previous studies investigating the downregulation of the $Na_v1.8$ current and expression in injured neurons (3,9,14). $Na_v1.8$ mRNA transcript and protein levels were significantly reduced in injured DRGs from 7 days after CCI and the current density mediated by the $Na_v1.8$ channel was markedly reduced at 21 days. However, it remains to be elucidated how this contributes to the neuropathic pain phenotype. Recently, emerging evidence has revealed that the increase in $Na_v1.8$ levels and TTX-R current upregulated in adjacent spared uninjured neurons may provide a reasonable explanation for the role of the $Na_v1.8$ channel in neuropathic pain models (12-14). However, in the present study, the current and expression of $Na_v1.8$ were not affected in contralateral uninjured DRGs. This indicated that there were no redistributed compensatory effects of $Na_v1.8$ in the contralateral uninjured DRGs under CCI-induced neuropathic pain, contrasting with previous studies (15).

A potential reason for the downregulation of the $Na_v1.8$ sodium channel is that the surgical procedure caused neuronal damage. During the present study, it was demonstrated that, in ipsilateral DRGs, CCI treatment induced neuronal damage in a time-dependent manner, exhibiting pyknosis and anachromasis of the nuclei as well as necrosis and shrunken cavities in the cell bodies. Similarly to behavioral assessments, the histological morphology of the contralateral DRGs remained unchanged among groups. It was hypothesized that the quantity of normal neurons affects the excitability of afferent neurons. Thus, functional analysis was performed using the patch clamp electrophysiological technique. It was identified that CCI treatment caused a depolarizing shift in the $Na_v1.8$ steady-state activation curve. This finding is supported by a previous study in which Amm VIII, an α-toxin isolated from venom, is able to induce rapid mechanical and thermal pain hypersensitivities by negatively shifting the activation curve (30). The slowly inactivating $Na_v1.8$ current has been observed to be capable of generating repeated action potentials (31). In the present study, a positive shift was also observed in the $Na_v1.8$ activation curve following the induction of CCI. This may induce the fast inactivated state and increase action potential firing rates.

Another neuronal TTX-R channel, $Na_v1.9$, has also been observed to be associated with neuropathic pain. A previous study revealed that $Na_v1.9$ expression decreased ~3.6 fold

under sciatic nerve ligation-induced neuropathic pain (15). However, during the present study, CCI-treatment only led to a significant decrease in the level of $Na_v1.9$ mRNA in DRGs ipsilateral to the injury. In addition, it is important to acknowledge that no change in the relative expression of $Na_v1.9$ protein and $Na_v1.9$ current density and dynamics were observed. This was conflicting with the normal behavior observed in the $Na_v1.9$ knockout mouse following CCI treatment (2). The reasons for this discrepancy remain to be elucidated at present and require further study.

In conclusion, the present study provided evidence of a role for $Na_v1.8$ in the pathogenesis of neuropathic pain. Of note, a positive shift of intact $Na_v1.8$ sodium channels in the DRG neurons ipsilateral to the induced injury was likely to have promoted ectopic discharge, rather than a compensatory regulation of contralateral uninjured DRG neurons.

References

1. Dib-Hajj SD, Binshtok AM, Cummins TR, Jarvis MF, Samad T and Zimmermann K: Voltage-gated sodium channels in pain states: role in pathophysiology and targets for treatment. Brain Res Rev 60: 65-83, 2009.
2. Leo S, D'Hooge R and Meert T: Exploring the role of nociceptor-specific sodium channels in pain transmission using Nav1.8 and Nav1.9 knockout mice. Behav Brain Res 208: 149-157, 2010.
3. Amir R, Kocsis JD and Devor M: Multiple interacting sites of ectopic spike electrogenesis in primary sensory neurons. J Neurosci 25: 2576-2585, 2005.
4. Joshi SK, Honore P, Hernandez G, et al: Additive antinociceptive effects of the selective Nav1.8 blocker A-803467 and selective TRPV1 antagonists in rat inflammatory and neuropathic pain models. J Pain 10: 306-315, 2009.
5. Amaya F, Decosterd I, Samad TA, et al: Diversity of expression of the sensory neuron-specific TTX-resistant voltage-gated sodium ion channels SNS and SNS2. Mol Cell Neurosci 15: 331-342, 2000.
6. Ho C and O'Leary ME: Single-cell analysis of sodium channel expression in dorsal root ganglion neurons. Mol Cell Neurosci 46: 159-166, 2011.
7. Blair NT and Bean BP: Roles of tetrodotoxin (TTX)-sensitive Na^+ current, TTX-resistant Na^+ current, and Ca^{2+} current in the action potentials of nociceptive sensory neurons. J Neurosci 22: 10277-10290, 2002.
8. Herzog RI, Cummins TR and Waxman SG: Persistent TTX-resistant Na^+ current affects resting potential and response to depolarization in simulated spinal sensory neurons. J Neurophysiol 86: 1351-1364, 2001.
9. Dib-Hajj S, Black JA, Felts P and Waxman SG: Down-regulation of transcripts for Na channel α-SNS in spinal sensory neurons following axotomy. Proc Natl Acad Sci USA 93: 14950-14954, 1996.
10. Chen X, Pang RP, Shen KF, Zimmermann M, Xin WJ, Li YY and Liu XG: TNF-α enhances the currents of voltage gated sodium channels in uninjured dorsal root ganglion neurons following motor nerve injury. Exp Neurol 227: 279-286, 2011.
11. Lai J, Gold MS, Kim CS, Bian D, Ossipov MH, Hunter JC and Porreca F: Inhibition of neuropathic pain by decreased expression of the tetrodotoxin-resistant sodium channel, NaV1.8. Pain 95: 143-152, 2002.

12. Gold MS, Weinreich D, Kim CS, Wang R, Treanor J, Porreca F and Lai J: Redistribution of Na(V)1.8 in uninjured axons enables neuropathic pain. J Neurosci 23: 158-166, 2003.
13. Zhang XF, Zhu CZ, Thimmapaya R, *et al*: Differential action potentials and firing patterns in injured and uninjured small dorsal root ganglion neurons after nerve injury. Brain Res 1009: 147-158, 2004.
14. Decosterd I, Ji RR, Abdi S, *et al*: The pattern of expression of the voltage-gated sodium channels Na(v)1.8 and Na(v)1.9 does not change in uninjured primary sensory neurons in experimental neuropathic pain models. Pain 96: 269-277, 2002.
15. Wang H, Sun H, Della Penna K, *et al*: Chronic neuropathic pain is accompanied by global changes in gene expression and shares pathobiology with neurodegenerative diseases. Neuroscience 114: 529-546, 2002.
16. Berta T, Poirot O, Pertin M, Ji RR, Kellenberger S and Decosterd I: Transcriptional and functional profiles of voltage-gated Na$^{(+)}$ channels in injured and non-injured DRG neurons in the SNI model of neuropathic pain. Mol Cell Neurosci 37: 196-208, 2008.
17. Sleeper AA, Cummins TR, Dib-Hajj SD, *et al*: Changes in expression of two tetrodotoxin-resistant sodium channels and their currents in dorsal root ganglion neurons after sciatic nerve injury but not rhizotomy. J Neurosci 20: 7279-7289, 2000.
18. Yu YQ, Zhao F, Guan SM and Chen J: Antisense-mediated knockdown of Na(V)1.8, but not Na(V)1.9, generates inhibitory effects on complete Freund's adjuvant-induced inflammatory pain in rat. PloS ONE 6: e19865, 2011.
19. Bennett GJ and Xie YK: A peripheral mononeuropathy in rat that produces disorders of pain sensation like those seen in man. Pain 33: 87-107, 1988.
20. Li X, Kang L, Li G, *et al*: Intrathecal leptin inhibits expression of the P2X2/3 receptors and alleviates neuropathic pain induced by chronic constriction sciatic nerve injury. Mol Pain 9: 65-73, 2013.
21. Lu Y and Westlund KN: Gabapentin attenuates nociceptive behaviors in an acute arthritis model in rats. J Pharmacol Exp Ther 290: 214-219, 1999.
22. Gao YH, Chen SP, Wang JY, Qiao LN, Meng FY, Xu QL and Liu JL: Differential proteomics analysis of the analgesic effect of electroacupuncture intervention in the hippocampus following neuropathic pain in rats. BMC Complement Altern Med 12: 241-251, 2012.
23. Tu WZ, Cheng RD, Cheng B, *et al*: Analgesic effect of electroacupuncture on chronic neuropathic pain mediated by P2X3 receptors in rat dorsal root ganglion neurons. Neurochem Int 60: 379-386, 2012.
24. Qiu F, Jiang Y, Zhang H, Liu Y and Mi W: Increased expression of tetrodotoxin-resistant sodium channels Nav1.8 and Nav1.9 within dorsal root ganglia in a rat model of bone cancer pain. Neurosci Lett 512: 61-66, 2012.
25. Maingret F, Coste B, Padilla F, Clerc N, Crest M, Korogod SM and Delmas P: Inflammatory mediators increase Nav1.9 current and excitability in nociceptors through a coincident detection mechanism. J Gen Physiol 131: 211-225, 2008.
26. McKay Hart A, Brannstrom T, Wiberg M, Terenghi G: Primary sensory neurons and satellite cells after peripheral axotomy in the adult rat: timecourse of cell death and elimination. Exp Brain Res 142: 308-318, 2002.
27. Ueda H: Molecular mechanisms of neuropathic pain-phenotypic switch and initiation mechanisms. Pharmacol Ther 109: 57-77, 2006.
28. Latremoliere A and Woolf CJ: Central sensitization: a generator of pain hypersensitivity by central neural plasticity. J Pain 10: 895-926, 2009.
29. Zhao ZQ: Neural mechanism underlying acupuncture analgesia. Prog Neurobiol 85: 355-375, 2008.
30. Abbas N, Gaudioso-Tyzra C, Bonnet C, *et al*: The scorpion toxin Amm VIII induces pain hypersensitivity through gain-of-function of TTX-sensitive Na$^+$ channels. Pain 154: 1204-1215, 2013.
31. Garrison SR, Weyer AD, Barabas ME, Beutler BA and Stucky CL: A gain-of-function voltage-gated sodium channel 1.8 mutation drives intense hyperexcitability of A- and C-fiber neurons. Pain 155: 896-905, 2014.